

Feedforward and State-Feedback Force-Position Control of a Robotic Platform Devoted to Precise Co-manipulation

Mourad BENOUSAAD^{1*}, Abdallah HABBADI¹, Mohammad AL JANAIDEH² and Micky RAKOTONDRABE¹

Abstract—This study deals with the precise co-manipulation of flexible object using a dual 1-dof robotic platform with nonlinear actuation. First, a mechanical model that considers the flexible object deformation with two robots nonlinearities is proposed. Then a feedforward-feedback control scheme is given to compensate for the nonlinearities and to stabilize the dynamics. Finally, simulation results with analysis are carried out to demonstrate the efficiency of the designed controllers.

I. INTRODUCTION

Object precise co-manipulation task using dual arm robots is essential in many robotics applications. It still remain a challenging research considering the coordination and the physical interaction between the two arms [1]. These complexity and issues arise when the manipulated objects are flexible and present a possibility of deformation as the stability of the entire task is strongly compromised. Objects flexibility can be found in several robotics applications: surgical robotics (organs and biological tissues manipulation), Industrial robotics application (manipulation of cable, textile, electronics component, or rubber components) and robotics for food industry (fruit and vegetable manipulation).

Several aspects and issues related to flexible objects manipulation were addressed ([2], [3], [4], [5], [6]): Type of used end-effectors (grripper or multi-fingered hand), sensing classification (force, position) and measurement approach (direct, vision-based, model-based), modeling and the control law strategies. Furthermore, other works considered co-manipulation of a flexible objects using two robots that implies a physical interaction ([7], [8], [9], [10], [11]). This physical interaction poses some problems related to the coordination between the two robots, the lack of object behavior knowledge under a physical constraints and the presence of nonlinearities in the object or in the actuators behaviors. For instance, in [9], authors considered the master-slave synchronization for handling coordination problem and by using a compliant robot control, while an overview of force control strategies were presented in [11]. In the same context, others robotic control strategies were explored such as PD combined with gravity compensation [7], robust control using slow and fast subsystems properties [10] and sliding mode control to handle uncertainty [8]. In most existing works, the flexible object model is not included in

the robotic control law and often the nonlinearities of object and actuators behaviors are not considered.

Similarly to larger sized objects, manipulation of smaller objects suffers from the same issues and limitations. In [12], [13], [14], different control strategies for two miniaturized manipulators handling small sized objects have been proposed but these latter were not flexible and thus tasks stability was not an important issue. In the current work, we explore the co-manipulation of highly flexible object through two manipulators. Against the above literature, this paper proposes to consider the model of the flexible model and takes it into account in the control strategy such that tasks stability be ensured whilst certain performances (response time, accuracy, disturbance rejection...) could be reached. Beyond the flexible objects characteristics consideration, we also account for the nonlinearity within the manipulators that we envisage to be based on piezoelectric materials. Simulation with various situations are carried out to demonstrate the efficiency of the proposed co-manipulation modeling and control.

The article is organised as follows. In Section II, the robotic platform and its model, including the object model, are first described. Then, in Section III, the proposed nonlinear control strategy is established and described. Simulation results are presented and discussed in Section IV. Finally Section V provides conclusions of this work and some perspectives.

II. PRESENTATION OF THE PLATFORM AND MODELING

A. Presentation of the platform

Within the context of the IPHRIMOB project, the final objective is to assemble two objects, at least one being flexible, thanks to the collaboration between one robot and a human, Fig.1. The robotic arm has an end-effector which is a pluri-digit hand, i.e. a hand with multiple fingers. Whilst the robotic arm is used to perform long distance movement (for instance for picking the object from the storage to the assembly area), the hand itself is used for fine assembly and positioning task. In this study, the hand at the terminal of the robotic arm is based on two linear digits/fingers that we will call manipulators in the sequel. We chose the two manipulators that compose the robotic hand to be based on piezoelectric actuators because of their high resolution and high bandwidth performances. The target of this paper is to model the robotic hand with the manipulated flexible object and to design control strategy such that both the manipulation force F_m and the fine positioning x_2 be controlled.

¹ Laboratoire Génie de Production, ENIT / Toulouse INP, University of Toulouse, Tarbes, France.

² Department of Mechanical Engineering, Memorial University, St. John's, Newfoundland, Canada.

*corresponding author, mourad.benoussaad@enit.fr

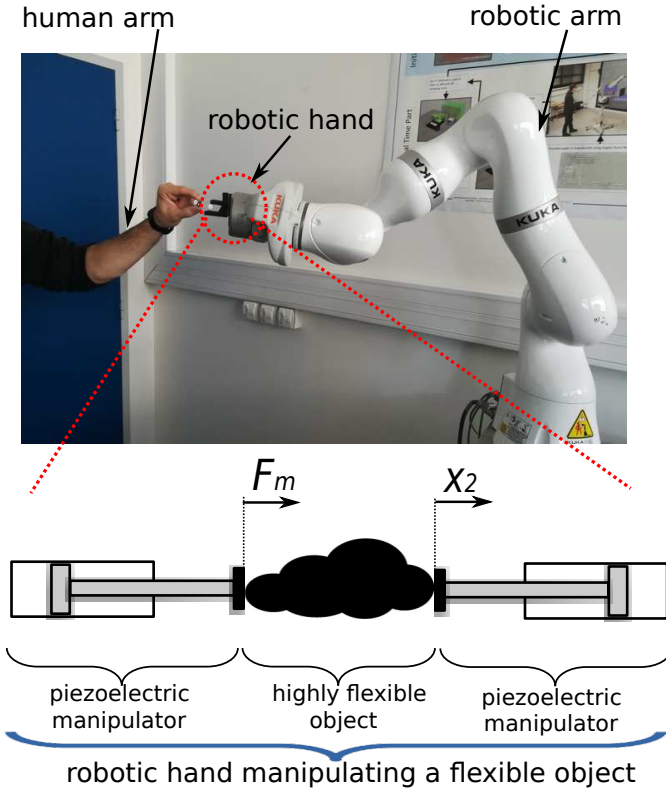


Fig. 1. Experimental setup of the human-robotic collaboration of the IPHRIMOB project.

B. Modeling

The robotic hand that manipulates an object illustrated in Fig.1 can be characterized by a set of three mass-damper-spring systems as shown in Fig.2. In this system the two manipulators are considered similar and having a second order dynamics behavior and a nonlinear part due to hysteresis phenomenon in the piezoelectric actuation. The flexible object can be characterized as a second order linear mass-spring-damper system. From Fig. 2, we derive the following

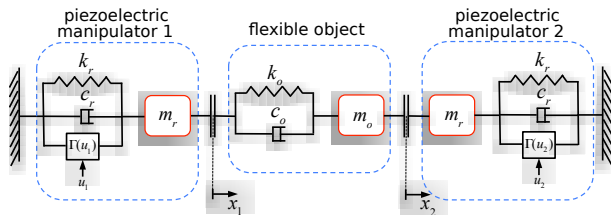


Fig. 2. Mechanical model of the manipulators and flexible object.

differential equations as

$$\begin{cases} m_r \ddot{x}_1 = (u_1) & k_r x_1 & c_r \dot{x}_1 + k_o(x_2 - x_1) + c_o(\dot{x}_2 - \dot{x}_1), \\ (m_r + m_o) \ddot{x}_2 = (u_2) & k_r x_2 & c_r \dot{x}_2 & k_o(x_2 - x_1) & c_o(\dot{x}_2 - \dot{x}_1), \\ F_m = & (k_o(x_2 - x_1) + c_o(\dot{x}_2 - \dot{x}_1)), \end{cases} \quad (1)$$

where u_i for $i \in \{1, 2\}$ is the driving voltage of the piezoelectric actuators in the manipulators, x_i is the displacement of each manipulator, F_m is the manipulation force applied by the manipulator-1 to the object, and $\Gamma(u_i)$ ($i \in \{1, 2\}$) is the hysteresis nonlinearity. The parameters k_j , c_j and m_j

($j \in \{r, o\}$) are the stiffness, the damping ratio, and the mass of the manipulators and the object.

Considering intermediary inputs $r_i(t) = \Gamma(u_i(t))$, we derive the following linear state-space model between the state $X(t)$, the input intermediary $r(t)$ and the output $Y(t)$:

$$\begin{cases} \frac{dX}{dt} = AX + Br \\ Y = CX \end{cases} \quad (2)$$

with:

$$\begin{aligned} X &= (x_1 \quad \dot{x}_1 \quad x_2 \quad \dot{x}_2)^T \\ Y &= (x_2 \quad F_m)^T \\ r &= (r_1 \quad r_2)^T \end{aligned} \quad (3)$$

where the state-matrix A , the input matrix B and the output matrix C are respectively:

$$\begin{aligned} A &= \begin{pmatrix} 0 & 1 & 0 & 0 \\ \frac{(k_o+k_r)}{m_r} & \frac{(c_o+c_r)}{m_r} & \frac{k_o}{m_r} & \frac{c_o}{m_r} \\ 0 & 0 & 0 & 1 \\ \frac{k_o}{(m_o+m_r)} & \frac{c_o}{(m_o+m_r)} & \frac{(k_o+k_r)}{(m_o+m_r)} & \frac{(c_o+c_r)}{(m_o+m_r)} \end{pmatrix} \\ B &= \begin{pmatrix} 0 & 0 \\ \frac{1}{m_r} & 0 \\ 0 & 0 \\ 0 & \frac{1}{(m_o+m_r)} \end{pmatrix} ; \quad C = \begin{pmatrix} 0 & 0 & 1 & 0 \\ k_o & c_o & k_o & c_o \end{pmatrix} \end{aligned} \quad (4)$$

We therefore have a Hammerstein structure, i.e. a linear dynamics that is represented by the state-space model in Eq 2 preceded by a static nonlinearity $r_i(t) = \Gamma(u_i(t))$. The related block diagram is presented in Fig.3.

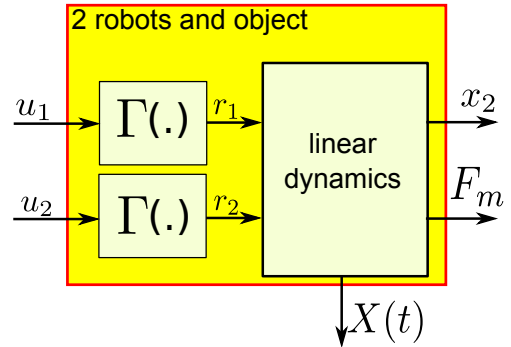


Fig. 3. Block diagram of the two manipulators and of the object.

III. FEEDFORWARD AND STATE-FEEDBACK CONTROL

In this section, we propose a controllers strategy that will permit to control the piezoelectric manipulator-2 of Fig.2 in position and the piezoelectric manipulator-1 in force. The aim is that the manipulator-2 is positioning very precisely the object whilst the other keeps it with a given manipulation force. The desired manipulation force is such that the object does not fall and in the same time its destruction due to possible larger force is avoided. Due to the hysteresis nonlinearity $r_i(t) = \Gamma(u_i(t))$ however, standard control technique for similar application cannot be employed. Therefore, we

suggest in this paper a combined feedforward-feedback control where the feedforward compensates for the hysteresis first, and the feedback is used to impose desired dynamics and to reduce any static error for accuracy perspective.

A. Hysteresis feedforward control

There are several hysteresis models in the literature many of which are used to approximate the nonlinear behaviors of smart materials based actuators and systems. Among these several models, few are exploited to feedforward control, i.e. control without feedback sensors. These include: the Preisach approach [15], [16], [17], the Bouc-Wen approach [18], [19], and the Prandtl-Ishlinskii (PI) approach [20], [21], [22]. The advantage of the PI approach is the implementation facility and accuracy modeling. In fact, a PI hysteresis model is represented by the superposition of several elementary and basic hysteresis called hysterons. The more one uses hysterons, the more the model accuracy will be. We therefore employ the PI approach in this paper.

Reconsider the hysteresis $r_i(t) = (u_i(t))$, with $i \in \{1, 2\}$ as shown in Fig. 3. Hence, the model is described by the following superposition of weighted hysterons as:

$$r_i(t) = (u_i(t)) = \sum_{k=1}^{n_h} w_k \gamma_k(u_i(t)), \quad (5)$$

where n_h is a positive integer presents the number of play operators, w_k are constants, and γ_k is a play operator [22]. Let $\eta_k^i(t) = \gamma_k(u_i(t))$, then the output of the play operator with the sampling time T_s is

$$\eta_k^i(t) = \max \{u_i(t) - s_k, \min \{u_i(t) + s_k, \eta_k^i(t - T_s)\}\}, \quad (6)$$

where s_k are positive thresholds determine the width of the hysteresis nonlinearities and with the initial condition is

$$\eta_k^i(0) = \max \{u_i(0) - s_k, \min \{u_i(0) + s_k, 0\}\}. \quad (7)$$

Note that the PI model in Eq 5 with hysterons in Eq 7 is called classical PI model. It is rate-independent, i.e. a static model, and is only accurate for symmetrical hysteresis. The identification of the above classical PI model from experimental data can be made with least-square minimisation method [23] or with a closed-form method [22]. To feedforward control a hysteresis nonlinearity that is modeled with the above classical PI model, a compensator $u_i(t) = c(r_{di}(t))$ is put in cascade with it as shown in Fig.4-a.

Two approaches exist to design the hysteresis compensator $u_i(t) = c(r_{di}(t))$ when dealing with a classical PI. In the first approach, the compensator $c(\cdot)$ is taken as another classical PI model with weightings and thresholds that are computed from the weightings and thresholds of the initial model (\cdot) [22]. In the second approach, the compensator $c(\cdot)$ is a re-arrangement of the initial model (\cdot) by using the inverse multiplicative structure [20], [24], [25]. An advantage of the second approach, which we will use, is that there is no additional computation of the compensator parameters: as soon as the initial model is identified, the compensator is derived through a re-arrangement of its

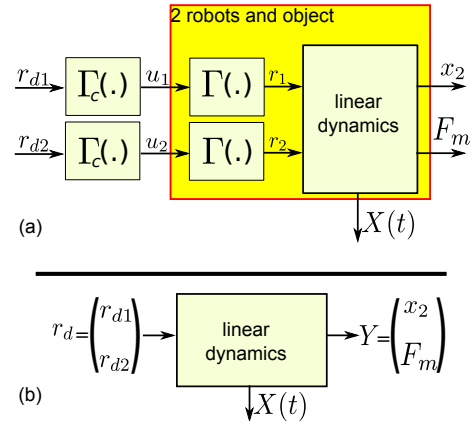


Fig. 4. The proposed feedforward control diagram.

structure. Thanks to this advantage, the inverse multiplicative structure has for instance been used in Bouc-Wen hysteresis compensation [18], Preisach hysteresis compensation [17] in rate-dependent PI hysteresis compensation [23], and in creep nonlinearity compensation [26].

The compensator of the hysteresis that is modeled with the classical PI in Eq 5 with hysterons in Eq 7 is therefore defined as follow [20], [25]:

$$u_i(t) = c(r_{di}(t)) = r_{di}(t) [(u_i(t - T_s)) \quad u_i(t - T_s)] \quad (8)$$

where $(u_i(t - T_s))$ is the initial model evaluated with the precedent value of u_i .

Once the hysteresis is compensated thanks to the compensator of Eq 8, we obtain a linear dynamic system. Hence, the nonlinear system preceded with the compensators shown in Fig 4-a is equivalent to the linear dynamic system of Fig 4-b. The new input is the vector r_d . Its model is given by Eq 9

$$\begin{cases} \frac{dX}{dt} = AX + Br_d \\ Y = CX \end{cases} \quad (9)$$

B. State-feedback control with poles assignment design

Subsection III-A presented the compensation of the hysteresis nonlinearity in the actuators. In this subsection, we add a feedback controller in order to impose desired dynamics for the manipulation task and in order to improve the tracking performance in term of accuracy. To this aim, we propose a state-feedback scheme as described in Fig.5, where K_c is the state-feedback gain and L is the prefilter, and where $Y_d = (x_{d2} \quad F_{dm})^T$ is the reference input composed of the desired position x_{d2} and the desired manipulation force F_{dm} .

Using the model in Eq 9 and using the control law $r_d(t) = LY_d(t) - K_c X(t)$ from Fig.5, we obtain the model of the closed-loop as follow:

$$\begin{cases} \frac{dX}{dt} = (A - BK_c) X + BLY_d \\ Y = CX \end{cases} \quad (10)$$

Eq 10 clearly reveals that the state matrix $(A - BK_c)$ of the closed-loop depends on the state-feedback gain K_c .

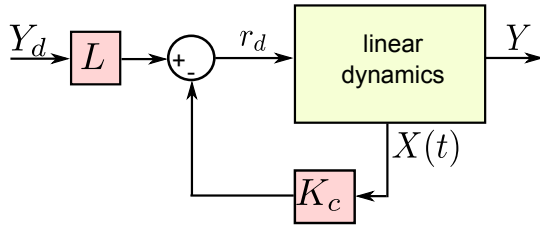


Fig. 5. The proposed feedforward-feedback control diagram.

Thus we can compute K_c such that $(A - BK_c)$ be Hurwitz (for stability) and have eigenvalues corresponding to some desired poles (for transient part performances). Such technique to compute K_c is called poles or eigenvalues assignment/placement technique. More precisely, if we impose desired eigenvalues as λ_{di} , $i \in \{1, 2, 3, 4\}$, our problem is:

Problem-1: Find K_c such that:

$(A - BK_c)$ is Hurwitz

$$\text{eig}(A - BK_c) = P_d = (\lambda_{d1} \ \lambda_{d2} \ \lambda_{d3} \ \lambda_{d4})^T$$

A way to numerically solve the eigenvalues assignment in **Problem-1** is through the well-known Ackermann's formula [27].

Once K_c is computed, the prefilter L can be obtained. To compute L , we first write the relationship between the output Y and the desired input Y_d at steady-state regime, which is obtained by letting all derivative in the model Eq 10 be equal zero, i.e. $\frac{dX}{dt} = 0$. This yields:

$$Y = C(BK_c - A)^{-1}BY_d. \quad (11)$$

To reach a zero static error, that is to let Eq 11 becomes $Y = Y_d$, the following condition on L should be satisfied:

$$L = \left(C(BK_c - A)^{-1}B \right)^{-1}. \quad (12)$$

IV. SIMULATION AND DISCUSSIONS

In this section, the above proposed feedforward-feedback control scheme and design is applied to the two piezoelectric manipulators grasping a flexible object. The implementation scheme is given by Fig.6 and various situations are studied in the simulation.

A. Numerical values of the model

The manipulated object characteristics are given in Table.I. The considered object is an O-ring shaped gasket classically used in watches to create an airtight seal that prevents water from entering through their crowns, made of rubber and with 5mm external diameter. The two manipulators, each actuated by a piezoelectric actuator, has linear dynamics of which parameters are also given in Table.I. The piezoelectric actuators are piezostacks which have high stiffness and thus have high force capability.

Parameters w_k and s_k of the nonlinear hysteresis part $r_i(t) = (u_i(t))$ of the piezoelectric actuators in the manipulators are based on the experimental data and identification in [20], [25]. Using 15 hysterons, we obtain Eq 13.

TABLE I
NUMERICAL VALUES.

Manipulated object		
equivalent mass	m_o	$1 \times 10^{-3}[kg]$
equivalent damping coefficient	c_o	$10[Ns/m]$
equivalent stiffness	k_o	$100[N/m]$
Left and right manipulators linear dynamics parameters		
equivalent mass	m_r	$13.2 \times 10^{-3}[kg]$
equivalent damping coefficient	c_r	$32.9[Ns/m]$
equivalent stiffness	k_r	$46053[N/m]$

$$\begin{aligned} (w_k) &= (43 \quad 3.95 \quad 1.17 \quad 6.57 \quad 2.07 \quad 2.52 \quad 6.05 \\ &\quad 1.5 \quad 2.65 \quad 2.29 \quad 2.07 \quad 3.81 \quad 4.11 \quad 2.56 \quad 22.8) \cdot 10^{-1} \\ (s_k) &= (0.07 \quad 0.32 \quad 0.74 \quad 1.3 \quad 2 \quad 2.8 \quad 3.67 \\ &\quad 4.61 \quad 5.54 \quad 6.5 \quad 7.34 \quad 8.1 \quad 8.8 \quad 9.3 \quad 9.7) \end{aligned} \quad (13)$$

B. Numerical values of the controllers

The compensator $u_i(t) = (r_{di}(t))$ has the same parameters than the initial model $r_i(t) = (u_i(t))$ which are the parameters given in Eq 13. Indeed the compensator is a re-arrangement of the model on the basis of the inverse multiplicative structure (see Eq 8). Regarding the feedback controllers parameters K_c and L , they are computed using **Problem-1** and Eq 12 respectively. To this, desired eigenvalues should be first imposed. There are several ways to chose desired eigenvalues. Meanwhile, we follow the next procedure:

i) the eigenvalues should have negative real to have Hurwitz $(A - BK_c)$, ii) they are chosen to have more stable eigenvalues of A , i.e. the better performance of the closed loop compared with the initial system. With more stable eigenvalues, we can obtain more rapid (= further negative in the real parts), less oscillations (= closer to zero in the imaginary parts), and iii) compute the controller gain K_c using the eigenvalues assignment in **Problem-1** and the Ackermann's formula, derive the prefilter L using Eq 12, and simulate the closed-loop,

iv) if the closed-loop performances are not satisfying, we modify the eigenvalues initially proposed in step-ii and re-start.

Finally, we propose the desired eigenvalues of $\lambda_{d1} = -30$, $\lambda_{d2} = -25$, $\lambda_{d3} = -12$, $\lambda_{d4} = -11$ for **Problem-1** and Eq 12, then we obtain:

$$\begin{aligned} K_c &= \begin{pmatrix} 46148 & 42 & 100 & 10 \\ 93 & 9 & 42889 & 39 \end{pmatrix} \\ L &= \begin{pmatrix} 3.928 & 0.0428 \\ 3.7485 & 0.00277 \end{pmatrix} \end{aligned} \quad (14)$$

C. Simulation with the controllers

The first simulation situation consists in performing a pick-transport-and-place task. To this aim, a desired manipulation force $F_m = 100mN$ is first applied at time $t = 1s$ in order to pick the object. Then, from $t = 2s$ to $t = 6s$, the object is moved at different place: a desired position $x_{d2} = 2mm$ is given to the closed-loop, then a new desired position $x_{d2} = -2mm$, and afterwards $x_{d2} = 0$. Finally,

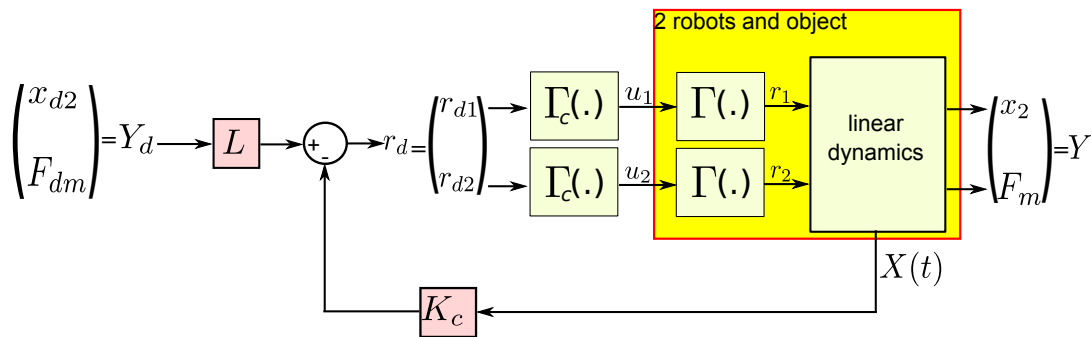


Fig. 6. Implementation of the feedforward-feedback control diagram.

the object is realized at $t = 8s$ by letting the manipulation force F_m be equal to zero. Fig. 7 gives the simulation result. The figure clearly demonstrates that during the transient-part (brusque change of desired force or position), the effect of the manipulation force (resp. the position) to the position (resp. manipulation force) is rapidly rejected. On the other hand, the curves reveal no oscillations and thus a "stable" manipulation and positioning task. A more analysis on the figures also shows that the response time on the positioning is of $318ms$ while the response time on the manipulation force is of $70ms$, the static errors in both are zero, and the overshoots are zero or negligible. Such performances are very interesting for the expected tasks in the project. In the second simulation, we consider a regulation situation

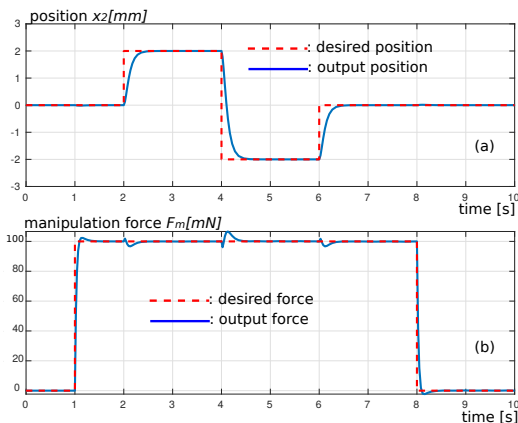


Fig. 7. The time history of Pick-transport-place situation. The figures show: (a) comparison between the desired position and output position, and (b) comparison between the desired force and output force.

where the object is hold at a desired position $x_{d2} = 0$ with a given manipulation force, and where an external disturbance is applied for perturbation. For that, a desired manipulation force $F_m = 100mN$ is first applied at $t = 1s$ to maintain the object. Then, at $t = 3s$, the manipulator-1 is disturbed which results in an undesired x_1 movement. At $t = 5s$, the manipulator-2 is also disturbed which results in an undesired x_2 movement. As from Fig.8, the effects of these two disturbances are quickly rejected both in the position of the object x_{d2} and in the manipulation force F_m . The results demonstrate the efficiency of the proposed controller to reject the external disturbance very quickly and

to maintain a "stable" manipulation task. An example of this situation is when one is performing a characterization or a machining on the grasped object, or when another object is being inserted in it.

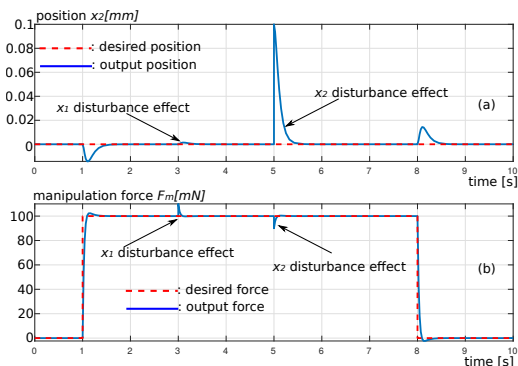


Fig. 8. The time history of position and manipulation force with external disturbances: (a) comparison between the desired position and output position, and (b) comparison between the desired force and output force.

D. Discussions

In order to ensure that the object be always kept within the two manipulators with the desired force whatever the position is, the response time on the manipulation force F_{dm} should be much quicker than that of the positioning x_{d2} . In our case, these response times are $70ms$ and $318ms$ respectively. This condition can only be satisfied by modifying the desired eigenvalues in the procedure in section IV-B.

As we can observe from Eq 1 and the related state-space representation, the model of the entire system strongly depends on the object characteristics. This is because we explicitly express the manipulation force evolution. This dependency is in fact valid whatever the used systems are: classical robotic systems [28] or miniaturized systems based on piezoelectric materials [12], [29].

In this paper, we proposed to consider the two manipulators with the manipulated object as one multivariable (two-inputs two-outputs) system. The controller is thus multivariable as well. However it is also possible to have an individual model (a single-input single-output, SISO) for each manipulator and to design a SISO controller for each of them separately. In these SISO cases, the effect of the left

(resp. right) manipulator to the right (resp. left) manipulator through the object is considered as external disturbance [12], [13], [14]. The advantage of working in a multivariable model and controller as suggested in this paper over SISO ones is the accuracy of the model, that is the cross-coupling between the two manipulators are taken into account in the modeling and therefore in the controller design.

The feedback part of the control strategy in this paper has a state-feedback architecture which requires that all the four states be available or measured. While the position x_1 and x_2 can be assumed to be measured with sensors, their derivative (velocities) \dot{x}_1 and \dot{x}_2 are not. Since we use piezoelectric actuators in the manipulators, piezoelectric self-sensing combined with observers [30] can be exploited to estimate these velocities.

V. CONCLUSIONS

We proposed the modeling and control of two piezoelectric actuators based manipulators in a robotic platform for precise manipulation of flexible objects. We first suggested a model that accounted for the nonlinearity and dynamics of the manipulators and the object deformation. Then a control strategy of the manipulation force and of the positioning has been proposed. Simulation results demonstrated the efficiency of the controller to perform precise and "stable" pick-and-place tasks with response times of 70ms and 318ms in force and in position respectively. The results were simulation and ongoing work consists of experimenting with the controller to the real platform system.

ACKNOWLEDGMENT

This work is supported by the IPHRIMOB-project (human-robotic physical interaction with biomechanic models) funded by the National Polytechnic Institute of Toulouse (Toulouse INP / ENIT).

REFERENCES

- [1] R. Herguedas, G. López-Nicolás, R. Aragüés, and C. Sagüés, "Survey on multi-robot manipulation of deformable objects," in *2019 24th IEEE International Conference on Emerging Technologies and Factory Automation (ETFA)*, pp. 977–984, 2019.
- [2] F. Khalil and P. Payeur, "Robotic manipulation of deformable objects with multi-sensory feedback - a review," *Robot Manipulators Trends and Development*, pp. 587–622, 2010.
- [3] F. Nadon, A. J. Valencia, and P. Payeur, "Multi-modal sensing and robotic manipulation of non-rigid objects: A survey," *Robotics*, vol. 7, no. 4, pp. 1–26, 2018.
- [4] D. Heirich and H. Wörn, eds., *Robot Manipulation of Deformable Objects*. Springer, 2000.
- [5] J. Sanchez, J.-A. Corrales, B.-C. Bouzgarrou, and Y. Mezouar, "Robotic manipulation and sensing of deformable objects in domestic and industrial applications: a survey," *The International Journal of Robotics Research*, vol. 37, no. 7, pp. 688–716, 2018.
- [6] F. Ruggiero et al., "Nonprehensile manipulation of deformable objects: Achievements and perspectives from the robotic dynamic manipulation project," *IEEE Robotics Automation Magazine*, vol. 25, no. 3, pp. 83–92, 2018.
- [7] D. Sun, J. K. Mills, and Y. Liu, "Position control of robot manipulators manipulating a flexible payload," *The International Journal of Robotics Research*, vol. 18, no. 3, pp. 319–332, 1999.
- [8] A. S. Al-Yahmadi, J. Abdo, and T. Hsia, "Modeling and control of two manipulators handling a flexible object," *Journal of the Franklin Institute*, vol. 344, no. 5, pp. 349–361, 2007.
- [9] H. Mkaouer and O. Boubaker, "Compliant motion control for handling a single object by two similar industrial robots," *Procedia Engineering*, vol. 41, pp. 1285–1291, 2012.
- [10] B. Esakki, R. B. Bhat, and C.-Y. Su, "Robust control of collaborative manipulators - flexible object system," *International Journal of Advanced Robotic Systems*, vol. 10, no. 5, pp. 1–18, 2013.
- [11] S. Flixeder, T. Glück, and A. Kugi, "Modeling and force control for the collaborative manipulation of deformable strip-like materials," *IFAC-PapersOnLine*, vol. 49, no. 21, pp. 95–102, 2016.
- [12] M. Rakotondrabe and I. A. Ivan, "Development and force/position control of a new hybrid thermo-piezoelectric microgripper dedicated to micromanipulation tasks," *IEEE Transactions on Automation Science and Engineering*, vol. 8, no. 4, pp. 824–834, 2011.
- [13] M. Rakotondrabe, J. Agnus, and P. Lutz, "Feedforward and imc-feedback control of a nonlinear 2-dof piezoactuator dedicated to automated micropositioning tasks," in *2011 IEEE International Conference on Automation Science and Engineering*, pp. 393–398, 2011.
- [14] S. Khadraoui, M. Rakotondrabe, and P. Lutz, "Interval force/position modeling and control of a microgripper composed of two collaborative piezoelectric actuators and its automation," *International Journal of Control, Automation and Systems*, vol. 12, no. 2, pp. 358–371, 2014.
- [15] P. Ge and M. Jouaneh, "Generalized Preisach model for hysteresis nonlinearity of piezoceramic actuators," *Precision engineering*, vol. 20, no. 2, pp. 99–111, 1997.
- [16] I. D. Mayergoyz, *Mathematical models of hysteresis and their applications*. New York: Elsevier Science, 2003.
- [17] R. Oubellil, L. Ryba, A. Voda, and M. Rakotondrabe, "Experimental model inverse-based hysteresis compensation on a piezoelectric actuator," in *2015 19th International Conference on System Theory, Control and Computing (ICSTCC)*, pp. 186–191, 2015.
- [18] D. Habineza, M. Rakotondrabe, and Y. Le Gorrec, "Multivariable generalized Bouc–Wen modeling, identification and feedforward control and its application to multi-dof piezoelectric actuators," *IFAC Proceedings Volumes*, vol. 47, no. 3, pp. 10952–10958, 2014.
- [19] J. Song and A. Der Kiureghian, "Generalized Bouc–Wen model for highly asymmetric hysteresis," *Journal of engineering mechanics*, vol. 132, no. 6, pp. 610–618, 2006.
- [20] M. Rakotondrabe, "Multivariable classical Prandtl–Ishlinskii hysteresis modeling and compensation and sensorless control of a nonlinear 2-dof piezoactuator," *Nonlinear Dynamics*, vol. 89, no. 1, pp. 481–499, 2017.
- [21] M. Al Janaideh and P. Krejčí, "Inverse rate-dependent Prandtl–Ishlinskii Model for feedforward compensation of hysteresis in a piezomicropositioning actuator," *IEEE/ASME Transactions on Mechatronics*, vol. 18, no. 5, pp. 1498–1507, 2013.
- [22] K. Kuhnen and H. Janocha, "Inverse feedforward controller for complex hysteretic nonlinearities in smart-material systems," *Control and Intelligent systems*, vol. 29, no. 3, pp. 74–83, 2001.
- [23] M. Al Janaideh, M. Rakotondrabe, I. Al-Darabsah, and O. Aljanaideh, "Internal model-based feedback control design for inversion-free feedforward rate-dependent hysteresis compensation of piezoelectric cantilever actuator," *Control Engineering Practice*, vol. 72, pp. 29–41, 2018.
- [24] O. Aljanaideh, M. Al Janaideh, and M. Rakotondrabe, "Inversion-free feedforward dynamic compensation of hysteresis nonlinearities in piezoelectric micro/nano-positioning actuators," in *2015 IEEE International Conference on Robotics and Automation (ICRA)*, pp. 2673–2678, 2015.
- [25] M. Rakotondrabe, "Classical prandtl-ishlinskii modeling and inverse multiplicative structure to compensate hysteresis in piezoactuators," in *2012 American Control Conference (ACC)*, pp. 1646–1651, 2012.
- [26] M. Rakotondrabe, "Modeling and compensation of multivariable creep in multi-dof piezoelectric actuators," in *2012 IEEE International Conference on Robotics and Automation (ICRA)*, pp. 4577–4581, 2012.
- [27] J. Ackermann, "Pole placement control," *Control System, Robotics and Automation*, vol. 8, no. 2011, pp. 74–101, 2009.
- [28] S. D. Eppinger and W. P. Seering, "On dynamic models of robot force control," *International Conference on Robotics and Automation*, pp. 29–34, 1986.
- [29] M. Rakotondrabe and Y. Le Gorrec, "Force control in piezoelectric microactuators using self scheduled H_∞ technique," *IFAC Proceedings Volumes*, vol. 43, no. 18, pp. 417–422, 2010.
- [30] M. Rakotondrabe, "Combining self-sensing with an unknown-input-observer to estimate the displacement, the force and the state in piezoelectric cantilevered actuators," in *2013 American Control Conference*, pp. 4516–4523, 2013.